JOURNAL OF MATERIALS SCIENCE 27 (1992) 6291–6298

A new parameter for describing the structure bifurcation in two-phase alloys containing coherent particles

M. DOI, T. MIYAZAKI
Department of Materials Science and Engineering, Metals Section, Nagoya Institute of Technology, Gokiso-Cho, Showa-Ku, Nagoya 466, Japan

The so-called bifurcation diagrams for γ' precipitate particles in nickel-based alloys were obtained by calculating the energy state for a pair of particles on the basis of the bifurcation theory. Based on the bifurcation diagrams, we have proposed a new parameter for describing the two-phase structure containing coherent particles. The parameter is defined as the mean particle radius at the intersection of the energy ridge and the line of $R=-0.5$ or $R=0.5$ in the bifurcation diagram ($R\equiv(r_\alpha-r_\beta)/(r_\alpha+r_\beta)$, where r_α and r_β are the radii of α and β), and is symbolized by $\bar{r}^*_{\pm 0.5}$. Because the energy state of the paired α and β is maximum at $\bar{r}^*_{\pm 0.5}$ when $R=\pm 0.5$, $\bar{r}^*_{\pm 0.5}$ is just like the watershed and hence we have termed it "structureshed". This parameter successfully describes the effects of elastic energy as well as surface energy on the microstructural changes during coarsening of precipitate particles.

1. Introduction

Our group has been studying the morphological changes of coherent precipitates not only by transmission electron microscopy (TEM) but also through theoretical calculations based on microelasticity theory, and has found several types of incredible behaviour of coherent precipitates during ageing of various nickel-based alloys [1–10]. Some typical examples of the behaviour are:

1. a single γ' (Ni_3X phase having $L1_2$ structure) cuboid splits into a pair of parallel small plates or eight small cuboids during coarsening;
2. coarsening of coherent particles slows down remarkably in the later stage of ageing;
3. coherent particles tend to become uniform in size during coarsening; and
4. coherent particles tend to exhibit a non-uniform distribution.

These phenomena are results of elastic energy and, in particular, of elastic interaction energy which arises from the overlap of elastic strain fields around coherent particles.

It used to be believed that the driving force for precipitate coarsening was the surface energy of precipitates. Coarsening due to surface energy is well-known as "Ostwald ripening". The theoretical treatments of Ostwald ripening are widely known as the "LSW theory" which was proposed by Lifschitz and Slyozov [11] and Wagner [12], or as "MLSW (Modified LSW) theories" which were obtained by modifying the LSW theory with respect to the volume fraction [13–19]. Some of the predictions of the above theories are

1. the mean particle radius $\bar{r}(t)$, at an ageing time, t, is proportional to $t^{1/m}$, i.e.

$$\bar{r}(t) = kt^{1/m} \quad (1)$$

where k and m are constant, and the so-called $t^{1/3}$ law holds (i.e. $m = 3$) provided the rate-controlling process is the lattice diffusion; and

2. the size-distribution of particles does not change during coarsening and can be scaled by $\bar{r}(t)$.

However, our findings are contradictory to the prediction of the already existing theories of coarsening. The contradiction is most likely to be due to the fact that the existing theories ignore the effect of elastic energy. Johnson [20–22] and our group [7, 23] have proposed a new theory of microstructural stability, named the "bifurcation theory" where the effects not only of surface energy but also of elastic energy are taken into consideration. Our new theory predicts that in elastically constrained systems, such as γ' particles in nickel-based alloys, smaller particles can coarsen at the expense of larger particles to produce a uniform structure; the bifurcation theory has brilliant expectations [10]. Kawasaki and Enomoto [24, 25] have studied the effects of elastic field interactions between precipitate droplets on the kinetics of Ostwald ripening. They showed theoretically the occurrence of the deceleration of particle coarsening, but their condition for calculating the elastic interaction energy is rather inconsistent with reality.

Our group also proposed the parameter Δ^* to describe the effect of elastic interaction energy on the γ' precipitate morphology in various nickel-based alloys [2, 3]. Δ^* is defined as the ratio of γ–γ' lattice

0022–2461

misfit to the surface energy density of γ' particle in γ matrix ($\Delta^* \equiv \delta/\gamma_S$). It is true that Δ^* is excellently used to describe the degree of elastic constraint and, in particular, the effects of elastic interaction energy, but Δ^* disregards the important point that elastic interaction depends on the inter-particle distance and hence the volume fraction of particles. We must find another parameter instead of Δ^* to describe the microstructural changes in coherent two-phase systems.

The aims of the present studies were:

1. to calculate the energy state of γ' particles in several nickel-based alloys by utilizing the bifurcation theory
2. to propose a new parameter which can describe the structure bifurcation in the systems containing coherent second-phase particles; and
3. to interpret the microstructural change during ageing of nickel-based alloys by utilizing the parameter newly proposed here.

2. Calculation based on stability bifurcation theory

2.1. Theoretical basis

The total free energy, E_{TTL} of the system containing coherent second-phase particles is expressed by the equation

$$E_{TTL} = E_{STR} + E_{INT} + E_{SURF} \quad (2)$$

where E_{STR} is the elastic strain energy due to δ, E_{INT} is the elastic interaction energy between particles, and E_{SURF} is the surface energy of particles; elastic energy, E_{ELA}, consists of E_{STR} and E_{INT}, i.e. $E_{ELA} = E_{STR} + E_{INT}$. Theoretically, the energy state of a two-phase structure should be calculated as a many-bodied problem because the structure usually contains a large number of particles, but in fact we cannot easily calculate the precise E_{INT} for more than two particles. Therefore, we calculate E_{TTL} for a pair of particles as the simplest case of a many-bodied problem.

Paired particles α and β are elastically inhomogeneous ellipsoids of revolution in an elastically anisotropic matrix. α and β change their sizes under the condition that their total volume remains constant. The constant volume, V, is expressed by the equation

$$V = (4\pi/3)(r_\alpha^3 + r_\beta^3) = 2(4\pi/3)\bar{r}^3 \quad (3)$$

The parameter R is used to describe the relative sizes of α and β, and is defined by the following equation proposed by Johnson [20]

$$R \equiv (r_\alpha - r_\beta)/(r_\alpha + r_\beta) \quad (4)$$

where r_α and r_β are the radii of α and β, respectively. R varies between -1 and 1 inclusive: when $R = 0$, both α and β are identical and take the mean radius $\bar{r}$; when $R = \pm 1$, only one of the pair exists and takes the maximum radius $2^{1/3}\bar{r}$. The volume fraction f_v, of paired particles is expressed by the equation

$$f_v = V/(2L^3) = \pi/(6d^3) \quad (5)$$

where d is obtained by normalizing the actual inter-particle distance L, with respect to the mean particle size $2\bar{r}$, i.e. $d \equiv L/(2\bar{r})$. Equation 4 indicates that f_v is determined only by d, regardless of V.

The total elastic strain energy, E_{STR}, of α and β is given by the equation

$$E_{STR} = E_{INCL}V_\alpha + E_{INCL}V_\beta \quad (6)$$

where V_α and V_β are the volumes of α and β, respectively. The elastic energy density, E_{INCL}, is calculated by using the following equation developed by Eshelby [26]

$$E_{INCL} = -(1/2)\sigma_{ij}^{I}e_{ij}^{T^*} \quad (7)$$

where σ_{ij}^{I} is the stress inside the particle and $e_{ij}^{T^*}$ is the eigenstrain, i.e. the stress-free strain or transformation strain. The elastic interaction energy, E_{INT}, between α and β is calculated using the following equation proposed by Yamauchi and de Fontaine [27]

$$E_{INT} = (1/v)\sum_{q} F^{\alpha\beta}(\boldsymbol{n})S^{\alpha}(\boldsymbol{q})S^{\beta}(-\boldsymbol{q})\exp(i\boldsymbol{q}\,\boldsymbol{L}) \quad (8)$$

where v is the volume of the system containing α and β, $\boldsymbol{n}$ is the unit vector along the Fourier wave-vector $\boldsymbol{q}$, $F^{\alpha\beta}(\boldsymbol{n})$ is the elastic energy coefficient in Fourier space, and $S^{\alpha}(\boldsymbol{q})$ and $S^{\beta}(-\boldsymbol{q})$ are the Fourier-space shape functions of α and β, respectively. The total surface energy, E_{SURF}, of α and β is calculated from the equation

$$E_{SURF} = \gamma_S(S_\alpha + S_\beta), \quad (9)$$

where S_α and S_β are the surface areas of α and β, respectively. The precise procedures for calculating the above energies are shown in our previous papers [1, 23].

2.2. Bifurcation diagrams

Fig. 1 shows a schematic diagram of the variation in the energy state, i.e. E_{TTL}, of paired coherent particles as a function of $\bar{r}$ and R. Fig. 2 is the so-called "bifurcation diagram" which is obtained by projecting the energy surface like Fig. 1 on to the $\bar{r}$–R plane. The bifurcation diagram is symmetric with respect to the line of $R = 0$. In both figures, each thick line indicates the energy ridge having the highest E_{TTL} at a given $\bar{r}$, while each broken line indicates the energy valley having the lowest E_{TTL} at a given $\bar{r}$. When $\bar{r}$ increases, the ridge branches at the point indicated by the triangle in Fig. 1 or 2. This junction is called the "bifurcation point". The part of the ridge on this side of the bifurcation point in Fig. 1 or on the right-hand side of the bifurcation point in Fig. 2, forms the boundary between Region I and Region II. In Region I, the energy minimum locates along $R = \pm 1$ and E_{TTL} decreases from the ridge ($R = 0$) to $R = \pm 1$ ($\bigcirc \rightarrow \bullet$) as indicated by thin arrows in Figs 1 and 2; on the contrary, in Region II the energy minimum locates along $R = 0$ and E_{TTL} decreases from the ridge to $R = 0$ ($\blacklozenge$) as indicated by bold arrows in Figs 1 and 2.

When $\bar{r}$ is small (e.g. at $\bar{r}_S$ in Figs 1 and 2), the state of paired α and β is in Region I where E_{SURF} is

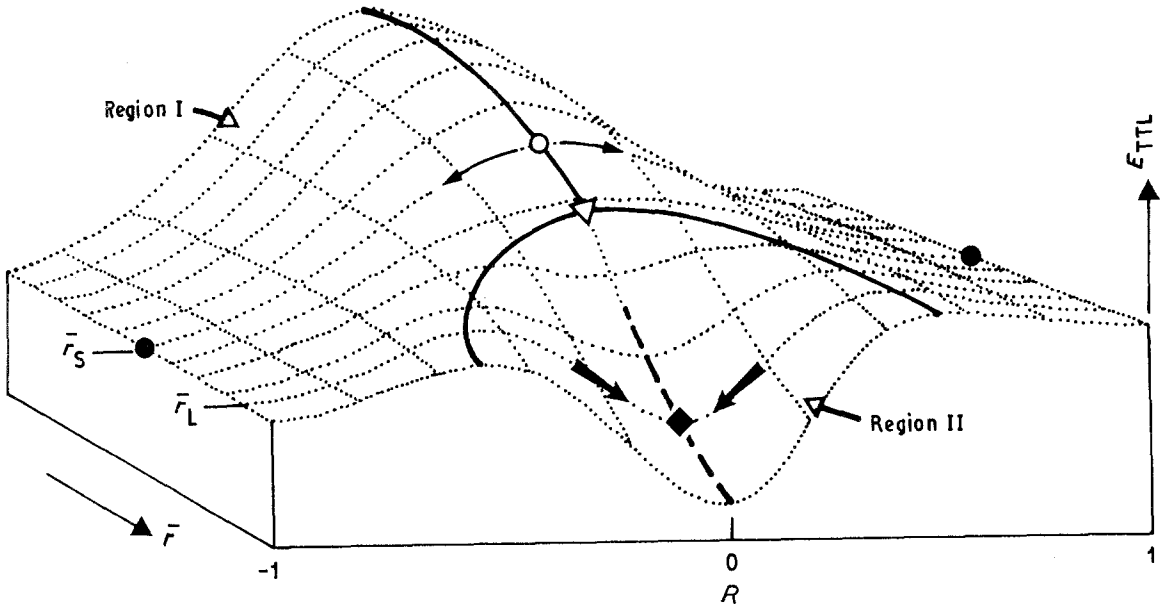

Figure 1 Schematic diagram of the energy state of paired coherent particles as a function of $\bar{r}$ and R, where $\bar{r}$ is the mean particle radius and R the parameter describing the relative sizes of the paired particles.

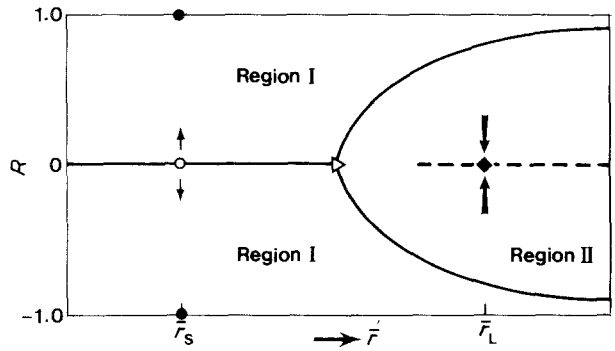

Figure 2 Schematic illustration of the so-called "bifurcation diagram" obtained by projecting the energy surface like Fig. 1 on to the $\bar{r}$–R plane. (——) The energy ridge having the maximum energy at a given $\bar{r}$, (— — —) the energy valley having the minimum energy at a given $\bar{r}$. In Region I, the surface energy is dominant; in Region II, the elastic energy is dominant and incredible coarsening behaviour can be expected.

dominant; the larger particle of the pair coarsens by absorbing the other and finally only one of the pair can stably exist. In Region I, microstructure coarsens to decrease E_{SURF} and hence E_{TTL}, as the conventional LSW and MLSW theories predicted. However, when $\bar{r}$ is large (e.g. at $\bar{r}_L$ in Figs 1 and 2), the state of paired α and β comes into Region II where E_{ELA} is dominant; the smaller particle of the pair coarsens by absorbing the other until both of the paired particles have the same size $\bar{r}$. This prediction for Region II surely corresponds to the incredible coarsening behaviour which we found, e.g. slowing down of coarsening, formation of uniform structure, etc.

Fig. 3a and b illustrate the bifurcation diagrams for γ′ particles in Ni–36.1% Cu–9.8%Si (all in at%) and Ni–47.4% Cu–5.0% Si alloys; the former is called Ni–Cu–Si(Hf) and the latter Ni–Cu–Si(Lf). Although these alloys have the same value of $|\delta|$ and also the same surface energy density γ_S ($\delta = -0.0129$ and $\gamma_S = 0.013\ J\,m^{-2}$), bifurcation diagrams differ from each

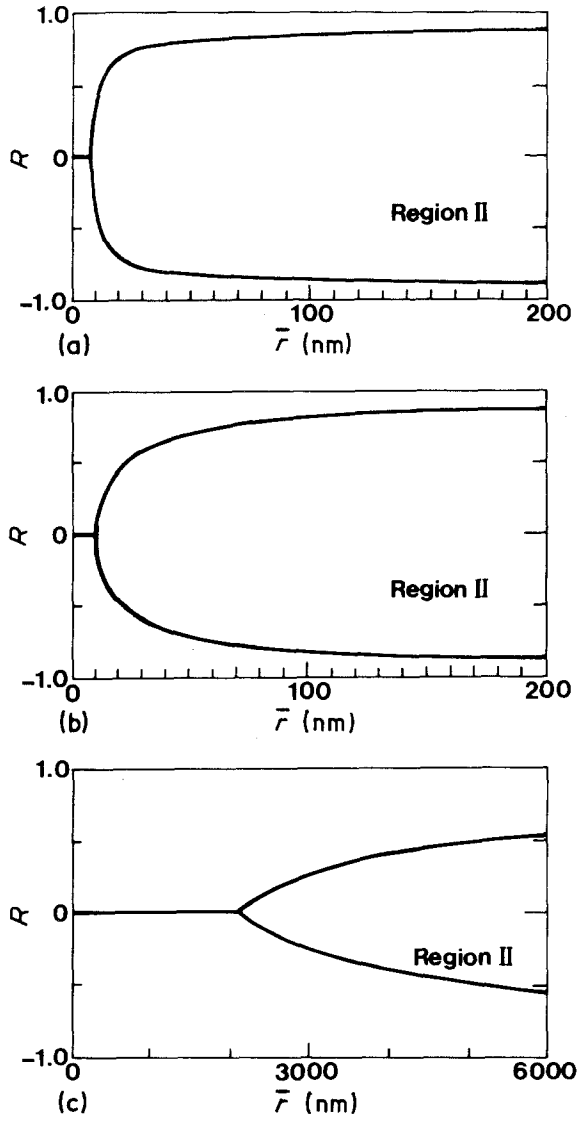

Figure 3 Bifurcation diagrams calculated for three nickel-based systems: (a) Ni–36.1%Cu–9.8%Si ($\delta = -0.0129$, $\gamma_S = 0.013\ J\,m^{-2}$, $f_v = 0.50$); (b) Ni–47.4%Cu–5.0%Si ($\delta = -0.0129$, $\gamma_S = 0.013\ J\,m^{-2}$, $f_v = 0.18$); (c) Ni–7.0%Si–6.0%Al ($\delta = 0.001$, $\gamma_S = 0.013\ J\,m^{-2}$, $f_v = 0.16$). The extent of Region II, where elastic energy is dominant, is governed by lattice misfit, surface energy and volume fraction.

other: Region II for Ni–Cu–Si(Hf) is wider than that for Ni–Cu–Si(Lf). This difference arises from the difference in volume fraction, f_v, of γ' particles. The f_v values are 0.50 for Ni–Cu–Si(Hf) and 0.18 for Ni–Cu–Si(Lf). Because f_v remains constant during coarsening at a given temperature for a given composition, the inter-particle distance, d, becomes shorter with increasing f_v. Elastic interaction becomes dominant with decreasing d. Hence the larger is f_v, the more dominant is the effect of elastic interaction. Actually, it is clear from Fig. 4 that the coarsening for larger f_v proceeds more slowly and slows down more easily than that for smaller f_v: $m = 5.8$ for Ni–Cu–Si(Hf) and $m = 3.6$ for Ni–Cu–Si(Lf).

Fig. 3c shows the bifurcation diagram for Ni–7.0% Si–6.0%Al alloy ($\delta = 0.001$, $\gamma_S = 0.013\ J\,m^{-2}$). Elastic energy originates from lattice misfit, δ. In Ni–Si–Al, the effects of elastic energy are negligibly small and the effect of surface energy is dominant because of small $|\delta|$. Therefore, the effect of elastic interaction in Ni–Cu–Si is much more dominant than that in Ni–Si–Al. Fig. 3 clearly indicates that Region II for large $|\delta|$ expands toward smaller $\bar{r}$ as compared with Region II for small $|\delta|$, that is, Region II becomes wider with increasing $|\delta|$. This means that even at small $\bar{r}$, the alloy system having large $|\delta|$ easily comes into the region where elastic energy is dominant.

3. A new parameter for describing structure bifurcation

Δ^* is a useful parameter for describing the effects of elastic interaction energy on the precipitate morphology [2, 3]. We can make good use of Δ^* when we compare the coarsening kinetics in Ni–Cu–Si ($\Delta^* = -1.0\ m^2\,J^{-1}$) with that in Ni–Si–Al ($\Delta^* = 0.07\ m^2\,J^{-1}$). The larger the value of $|\Delta^*|$, the more dominant is the elastic energy: the coarsening for larger $|\Delta^*|$ proceeds more slowly than that for smaller $|\Delta^*|$. When we compare two Ni–Cu–Si alloys, however, Δ^* is no longer effective. Although they have the same value of Δ^* ($\Delta^* = -1.0\ m^2\,J^{-1}$), their coarsening behaviours actually differ from each other. This difference arises from the fact that elastic interaction becomes more dominant with decreasing d and hence with increasing f_v. The bifurcation diagram includes the effect of f_v in addition to the effects of δ and γ_S. Fig. 3a and b clearly show the difference between the bifurcation diagrams for the two Ni–Cu–Si alloys. Hence the new parameter to be proposed should be based on the bifurcation diagram.

Considering the point that all types of the incredible behaviour of particle coarsening take place under the influence of elastic energy in Region II of the bifurcation diagram, we must find a new parameter which represents the extent of Region II. Fig. 5 schematically shows various types of bifurcation diagrams. A prospective candidate for the parameter is the bifurcation point indicated by triangles (Δ, ▲) in the figure. The point performs its duties fairly well as the parameter for describing the size limit to which particles should coarsen to enter Region II. On comparing (a) with (b) in the figure, however, the bifurcation point no longer works well for expressing the extent of Region II.

The parameter which we are now newly proposing is symbolized by $\bar{r}^*_{\pm 0.5}$. This point is defined as the $\bar{r}$ value at the intersection of the energy ridge and the line of $R = -0.5$ in the bifurcation diagram, e.g. □ and ■ in Fig. 5. The intersection of the energy ridge and the line of $R = 0.5$ also gives the same value of $\bar{r}^*_{\pm 0.5}$ because the bifurcation diagram is symmetric with respect to the line of $R = 0$. Because E_{TTL} decreases from $\bar{r}^*_{\pm 0.5}$ to the directions of smaller and larger $\bar{r}$ along $R = -0.5$ or $R = 0.5$, $\bar{r}^*_{\pm 0.5}$ is just like

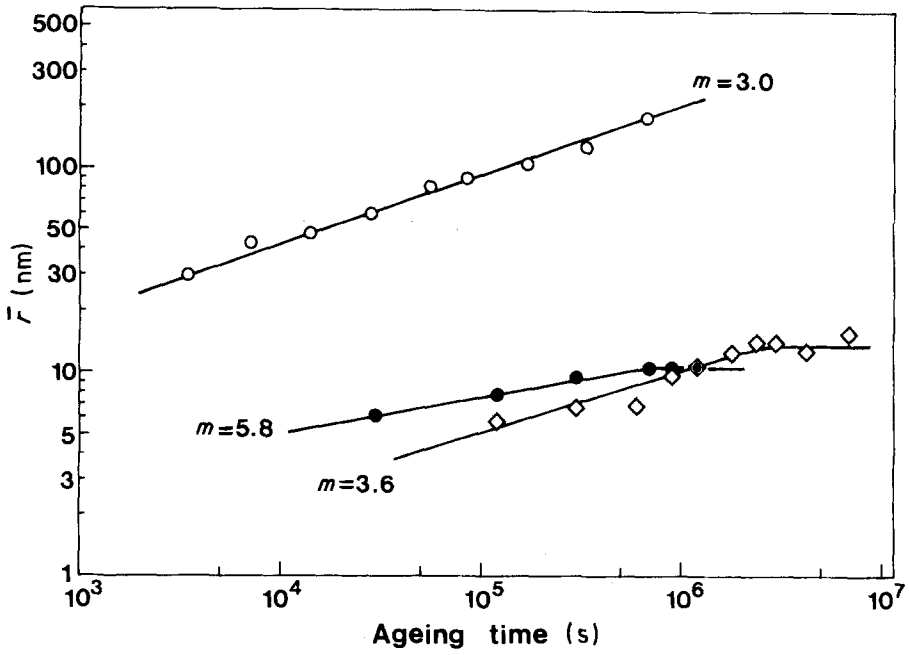

Figure 4 Coarsening kinetics of γ' particles in nickel-based alloys: (●) Ni–36.1%Cu–9.8%Si($\delta = -0.0129$, $\gamma_S = 0.013\ J\,m^{-2}$, $f_v = 0.50$); (◇) Ni–47.4% Cu–5.0%Si($\delta = -0.0129$, $\gamma_S = 0.013\ J\,m^{-2}$, $f_v = 0.18$); (○) Ni–7.0%Si–6.0%Al ($\delta = 0.001$, $\gamma_S = 0.013\ J\,m^{-2}$, $f_v = 0.16$). m value in the equation $\bar{r}(t) = Kt^{1/m}$ depends on lattice misfit, surface energy density and volume fraction.

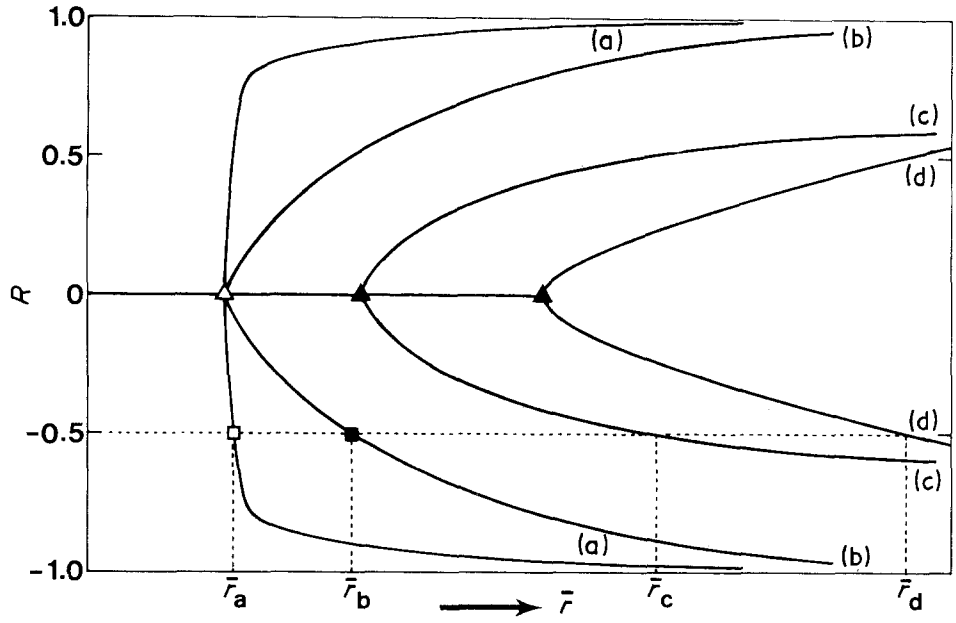

Figure 5 Schematic illustration of various types of bifurcation diagrams. The parameter structureshed ($\bar{r}^*_{\pm 0.5}$) is defined as the intersection of the energy ridge and the line of $R = -0.5$ (e.g. □, ■) or $R = 0.5$.

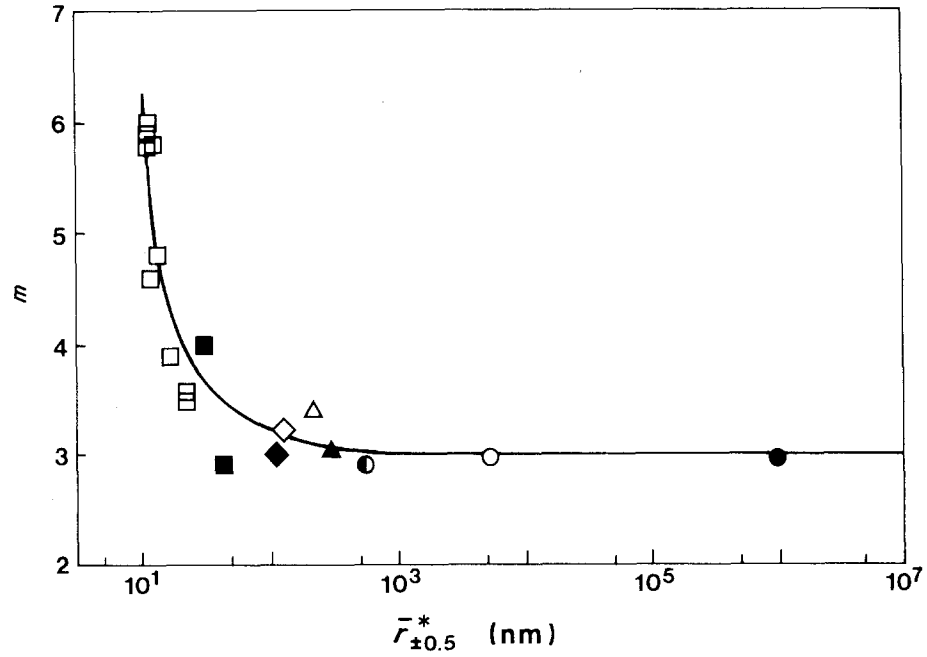

Figure 6 Correlation between structureshed $\bar{r}^*_{0.5}$ and m (in the equation $\bar{r}(t) = Kt^{1/m}$) for coherent particles in various alloy systems. (●) Ni–Cr–Al; (○) Ni–Si–Al; (◐) Cu–Co; (▲) Ni–Al; (△) Ni–Si; (◇) Ni–Mo; (◆) Ni–Ti; (■) Cu–Ti; (□) Ni–Cu–Si.

the watershed and we term it a "structureshed". Fig. 5 indicates that the values of $\bar{r}^*_{\pm 0.5}$ for (a) and (b) have different values, i.e. $\bar{r}_a$ (□) and $\bar{r}_b$ (■), respectively, although the bifurcation points are identical. The structureshed successfully expresses the difference in the extent of Region II. The usefulness of the parameter $\bar{r}^*_{\pm 0.5}$ in describing the coarsening behaviour of coherent precipitates will be shown in Section 4.

4. Interpretation of structural changes by utilizing the parameter "structureshed"

4.1. Coarsening kinetics

The experimentally obtained values of m and the calculated values of $\bar{r}^*_{\pm 0.5}$ are summarized for various alloy systems containing coherent particles in Table I. The data in Table I are plotted in a logarithmic scale in Fig. 6. This figure clearly indicates that there is a good correlation between structureshed ($\bar{r}^*_{\pm 0.5}$) and m value, as shown by the solid line. As $\bar{r}^*_{\pm 0.5}$ increases, m rapidly decreases and approaches 3, which is predicted by the conventional LSW or MLSW theories. In other words, as the effect of elastic interaction becomes weaker, the coarsening rate approaches that explained by LSW or MLSW theories; when the elastic interaction is dominant, the coarsening rate is very slow and deviates greatly from that predicted by LSW or MLSW theories. The structureshed parameter successfully describes the coarsening kinetics in elastically

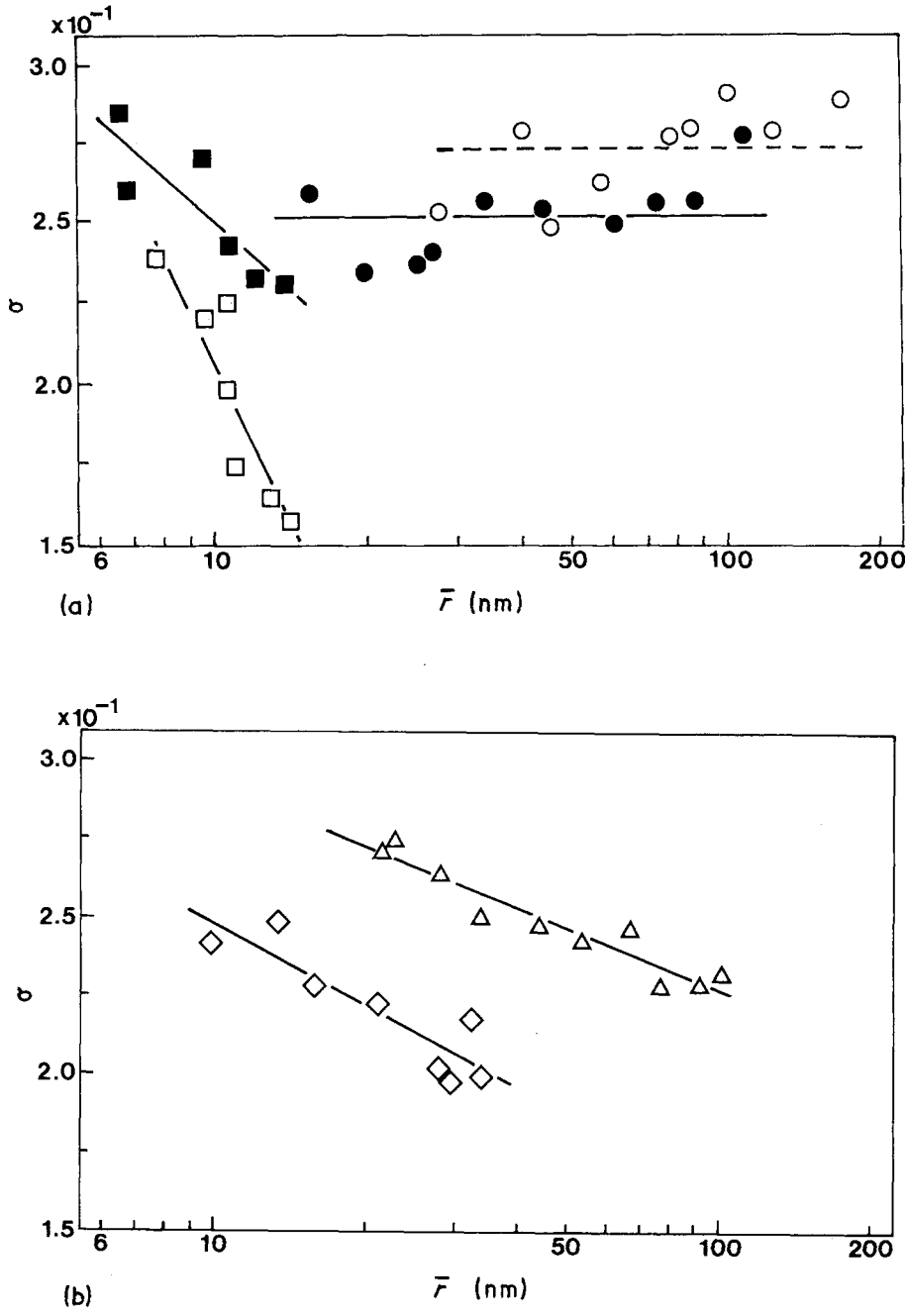

Figure 7 Variations in the standard deviation, σ, of size distribution during coarsening of coherent precipitates in various nickel-based alloys: Ni_4Mo particles in Ni–Mo alloy, γ′ in the other nickel-based alloys. (a) (○) Ni–7.0Si–6.0Al; (●) Ni–18.2Cr–6.2Al; (■) Nl–47.4Cu–5.0Si(Lf); (□) Ni–36.1Cu–9.8Si(Hf). (b) (△) Ni–15.4Si; (◇) Ni–16.3Mo.

constrained systems. In particular, the parameter can well express the effect of volume fraction and hence the effect of elastic interaction on the coarsening kinetics.

4.2. Change in the size distribution of particles

Fig. 7a and b illustrate the relation between the mean particle radius, $\bar{r}$ and the standard deviation, σ, of size distribution for γ′ or Ni_4Mo particles in various nickel-based alloys. During coarsening, σ values for some particles do not seriously change, and some particles exhibit a gradual decrease in σ, and others exhibit a rapid decrease. The decrease in σ means that the size distribution of particles becomes less scattered and hence particles become uniform in size. To express the rate of change in σ, we choose $d\log\sigma/d\log\bar{r}$. It is clear from Fig. 8 that there exists a good correlation between $\bar{r}^*_{\pm 0.5}$ and $d\log\sigma/d\log\bar{r}$, as shown by solid line. As $\bar{r}^*_{\pm 0.5}$ decreases from 10^3, $d\log\sigma/d\log\bar{r}$ rapidly decreases: as the elastic interaction becomes more dominant, σ decreases more rapidly and hence the two-phase structure becomes uniform more rapidly. The structureshed is also a good parameter which can excellently describe the effect of elastic energy on the size distribution of precipitate particles in elastically constrained systems.

5. Conclusion

There are many types of coarsening behaviour which cannot be explained by the conventional LSW or

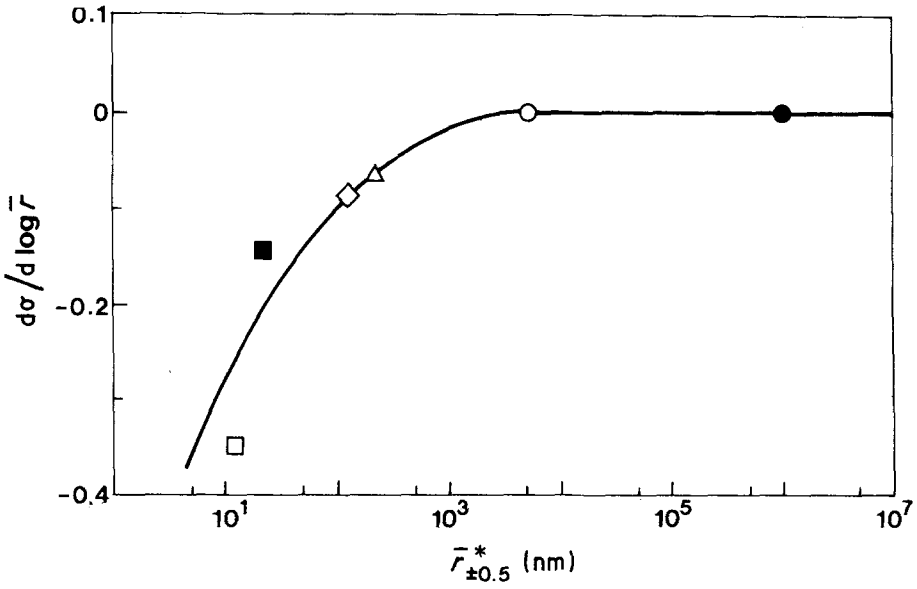

Figure 8 Correlation between structureshed ($\bar{r}^*_{\pm 0.5}$) and the rate of the change in standard deviation of size-distribution ($d\log\sigma/d\log\bar{r}$) for coherent precipitates in various nickel-based alloys. (●) Ni–Cr–Al; (○) Ni–Si–Al; (△) Ni–Si; (◇) Ni–Mo; (■) Ni–Cu–Si(Lf); (□) Ni–Cu–Si(Hf).

TABLE I Volume fraction, f_v, calculated values of structureshed $\bar{r}^*_{\pm 0.5}$, and experimentally obtained m values in the kinetic equation of coarsening, $\bar{r}(t) = Kt^{1/m}$, for coherent particles in various elastically constrained systems

Alloy system (at %)	f_v	$\bar{r}^*_{\pm 0.5}$ (nm)	m
Ni–18.2Cr–6.2Al	0.11	980000	2.96
Ni–7.0Si–6.0Al	0.16	5300	2.97
Cu–4.0Co [28]	0.036	561	2.9
Ni–12.5Al [8]	0.10	303	3.04
Ni–15.4Si	0.33	220	3.39
Ni–16.3Mo	0.48	124	3.22
Ni–10Ti [29]	0.22	112	3.0
Cu–4.18Ti	0.20	44	2.9
Cu–4.7Ti [30]	0.31	31	4.0
Ni–47.4Cu–5.0Si[a]	0.18	22	3.58
Ni–47.4Cu–5.0Si [31]	0.18	22	3.5
Ni–45.0Cu–6.0Si [31]	0.25	17	3.9
Ni–42.6Cu–7.0Si [31]	0.32	14	4.8
Ni–40.0Cu–8.0Si [31]	0.38	13	5.8
Ni–38.0Cu–9.0Si [31]	0.44	12	4.6
Ni–36.1Cu–9.8Si [31]	0.50	12	5.9, 6.0
Ni–36.1Cu–9.8Si[b]	0.50	12	5.78

[a] Ni–Cu–Si(Lf)
[b] Ni–Cu–Si(Hf)

MLSW theories of Ostwald ripening. It is becoming widely accepted that sometimes the effects of elastic energy and, in particular, of elastic interaction energy are actually dominant during coarsening of precipitates. In elastically constrained systems, such as γ' particles in a γ matrix, it is essential that we should specify not only the surface energy but also the lattice misfit and the volume fraction, because the latter two govern the elastic interaction. The structureshed ($\bar{r}^*_{\pm 0.5}$) which we have newly introduced here, is an excellent parameter for describing the structural changes in elastically constrained systems containing second-phase particles, whether the particles are coherent or incoherent.

Acknowledgements

The authors thank Dr T. Kozakai, Nagoya Institute of Technology, and Mr D. Konagaya, Nagoya Institute of Technology (now at the Honda Motor Co. Ltd) for assistance. Part of the present studies was financially supported by a Grant-in-Aid for Scientific Research from the Ministry of Education, Science and Culture, Japan.

References

1. T. MIYAZAKI, H. IMAMURA and T. KOZAKAI, *Mater. Sci. Engng* **54** (1982) 9.
2. M. DOI, T. MIYAZAKI and T. WAKATSUKI, *ibid.* **67** (1984) 247.
3. M. DOI and T. MIYAZAKI, in "Superalloys 1984", edited by M. Gell, C. S. Kortovich, R. H. Bricknell, W. B. Kent and J. F. Radavich (The Metallurgical Society, Warrendale, PA, 1984) p. 543.
4. M. DOI, T. MIYAZAKI and T. WAKATSUKI, *Mater. Sci. Engng* **74** (1985) 139.
5. M. DOI and T. MIYAZAKI, *ibid.* **78** (1986) 87.
6. M. DOI, T. MIYAZAKI, S. INOUE and T. KOZAKAI, in "Dynamics of Ordering Processes in Condensed Matter", edited by S. Komura and H. Furukawa (Plenum Press, New York, 1988) p. 287.
7. T. MIYAZAKI, M. DOI and T. KOZAKAI, *Solid State Phenom.* **3/4** (1988) 227.
8. M. DOI and T. MIYAZAKI, in "Superalloys 1988", edited by D. N. Duhl, G. Maurer, S. Antolovich, C. Lund and S. Reichman (The Metallurgical Society, Warrendale, PA, 1988) p. 663.
9. M. DOI, M. FUKAYA and T. MIYAZAKI, *Philos. Mag. A* **57** (1988) 821
10. T. MIYAZAKI and M. DOI, *Mater. Sci. Engng* **A110** (1989) 175.
11. I. M. LIFSHITZ and V. V. SLYOZOV, *J. Phys. Chem. Solids* **19** (1961) 35.
12. C. WAGNER, *Z. Elektrochem.* **65** (1961) 581.
13. A. J. ARDELL, *Acta Metall.* **20** (1972) 61.
14. A. D. BRAILSFORD and P. WINBLATT, *ibid.* **27** (1979) 489.
15. C. K. DAVIES, P. NASH and R. N. STEVENS, *ibid.* **28** (1980) 179.
16. K. TSUMURAYA and Y. MIYATA, *ibid.* **31** (1983) 437.

17. J. A. MARQUSEE and J. ROSS, *J. Chem. Phys.* **80** (1984) 536.
18. P. W. VOORHEES and M. E. GLICKSMAN, *Acta Metall.* **32** (1984) 2001.
19. Y. ENOMOTO, M. TOKUYAMA and K. KAWASAKI, *ibid.* **34** (1986) 2119.
20. W. C. JOHNSON, *ibid.* **32** (1984) 465.
21. W. C. JOHNSON and J. W. CAHN, *ibid.* **32** (1984) 1925.
22. W. C. JOHNSON and G. MARTIN, *Solid State Phenom.* **3/4** (1988) 247.
23. T. MIYAZAKI, K. SEKI, M. DOI and T. KOZAKAI, *Mater. Sci. Engng* **77** (1986) 125.
24. K. KAWASAKI and Y. ENOMOTO, *Physica A* **120** (1988) 463.
25. Y. ENOMOTO and K. KAWASAKI, *Acta Metall.* **37** (1989) 1399.
26. J. D. ESHELBY, *Prog. Solid Mech.* **2** (1961) 89.
27. H. YAMAUCHI and D. FONTAINE, *Acta Metall.* **27** (1979) 763.
28. Y. SENO, Y. TOMOKIYO, K. OKI and T. EGUCHI, *Trans. Jpn Inst. Metals* **24** (1983) 491.
29. H. SUGA, T. MIYAZAKI and E. YAJIMA, *J. Jpn Inst. Metals* **34** (1970) 1190.
30. T. MIYAZAKI, E. YAJIMA and H. SUGA, *ibid.* **34** (1970) 1184.
31. S. YOSHIDA, M. FUKAYA and T. MIYAZAKI, *ibid.* **51** (1987) 18.

Received 12 February 1990
and accepted 17 February 1992